

Whole-Body Continuously Moving Table Fat Water Imaging with Dynamic ΔB_0 Shimming

Saikat Sengupta^{1,2}, David S Smith^{1,2}, and E. Brian Welch^{1,2}

¹Radiology and Radiological Sciences, Vanderbilt University, Nashville, Tennessee, United States, ²Vanderbilt University Institute of Imaging Science, Nashville, Tennessee, United States

INTRODUCTION

The quantification of whole-body fat/water content is valuable in the staging and treatment planning of a number of disorders linked to obesity, diabetes and circulation (1). Multiecho MRI based fat/water quantification is a standard technique that can provide accurate, clinically relevant whole-body measurements of water and fat fractions (2). Additionally, whole-body MRI with a Continuously Moving Table (CMT) offers a powerful solution to achieve rapid fat/water quantification (3). However, unlike multistation whole-body scanning, a limitation of CMT MRI is that the center-frequency (f_0) and shim calibrations are performed at one location of the body (commonly, the abdomen) and maintained throughout the scan for the full field of view. This results in non-optimal and often damaging field settings in other sections of the body. This proves to be deleterious in fat/water quantification and can cause inaccurate separation of the chemical species, especially in locations where ΔB_0 is high such as the neck, shoulders and upper abdomen. In this work, we present a solution to this problem by dynamically shimming different locations of the body during a CMT scan with shim and f_0 settings optimal for each individual anatomical location. As a proof of principle, we demonstrate table-position-optimized shimming in 5 different locations of the body.

METHODS

Acquisition: Whole-body CMT MRI was implemented on a Philips Achieva 3 Tesla scanner (Philips Healthcare, The Netherlands) with a 2-channel receive body coil and table velocity of 20 mm/s. To estimate the ΔB_0 distribution prior to shimming, an initial 4-echo golden angle (GA) radial CMT MRI scan (4) was performed on an adult volunteer without any shims applied (No Shim image: **NS**). The f_0 calibration and other scan preparation phases were performed automatically by the scanner at the level of the abdomen. The other scan parameters were: Full zFOV = 1800 mm, in-plane, FOV = 400 x 400 mm², inplane resolution = 2.5 x 2.5 mm², TR = 6.6 ms, first TE/ Δ TE = 0.99/1.4 ms, excited slice thickness = 12 mm. The total acquisition time was 90 seconds.

Reconstruction: To estimate table-position-specific ΔB_0 shims, complex axial images of the four echoes were reconstructed offline for 5 selected slices (slice to be shimmed), and 2 slices superior and inferior to the selected slices (for through-plane corrections). The selected slices were at the level of the head (slice 50), shoulders (slice 160), upper abdomen (slice 230), lower abdomen (slice 300) and thighs (slice 430), locations where the ΔB_0 was expected to be significantly disparate. Reconstructions were performed in Python (Anaconda version 3.4.2., TX) with 128 profiles per slice ($128 * 20 \text{ mm/s} * 6.6 \text{ ms} = 16.9 \text{ mm slice thickness; slice separation} = 2.5 \text{ mm}$). GA image reconstruction involved correction for k -space shifts and sampling density prior to gridding, 2D FFT and roll-off compensation.

Water/Fat Separation and ΔB_0 Estimation: 2D water/fat separation and ΔB_0 estimation based on a multiscale whole-image optimization algorithm (5) implemented in C++ was performed for all the 15 selected slices. Fat was modeled using 9 peaks (6).

Dynamic ΔB_0 Shimming: 0th and 1st order (f_0 , X, Y, Z) shim corrections were estimated for the 5 selected slices using the set of three ΔB_0 maps centered at the slices of interest with the method outlined in (7). The multiecho scan was then repeated, with the slice optimized shims applied for the radial projections corresponding to these 5 slices (Dynamic Shim image: **DS**). 2D water/fat separation and ΔB_0 estimation was then repeated for this shimmed dataset.

RESULTS

Figure 1a and 1b show a whole-body image for echo 1 and the ΔB_0 map acquired in the **NS** case. As expected, the ΔB_0 varies significantly along the extent of the body, with sections such as the shoulders and upper abdomen having extreme field inhomogeneities. It is clear that a single shim setting would be non-optimal in this scenario, and possibly detrimental to the field in other slices. Figure 1c shows retrospectively calculated table-position-specific shim values for the whole-body affirming the need for table-position-specific shims. The 5 selected slices shimmed in the **DS** scan are marked by the dotted lines. Figure 2a compares ΔB_0 maps for the **NS** and the **DS** cases in the 5 slices. The ΔB_0 is reduced significantly in all the slices with **DS** compared to **NS**, with the residual field showing only higher order variations. Figure 2b displays the resulting fat/water separations for the **DS** scan.

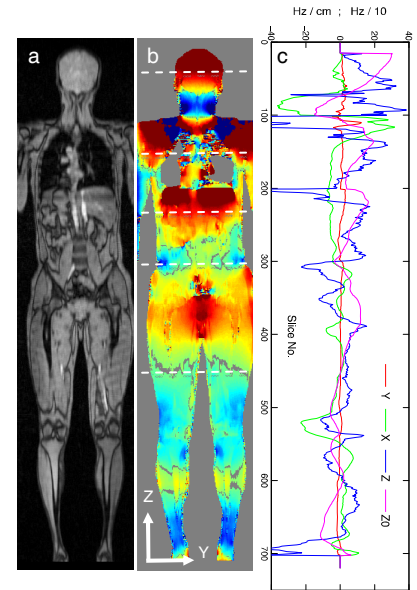


Figure 1: (a) Echo 1 Whole body image. (b) whole-body fieldmap without dynamic shims (c) Full body slice specific shims

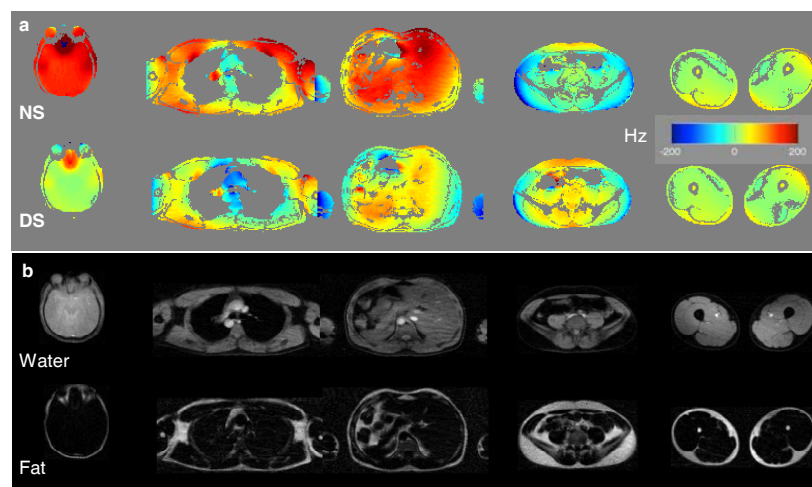


Figure 2(a): ΔB_0 fieldmaps of the 5 selected slices without shims (**NS**) and after Dynamic Shimming (**DS**). (b) Water/Fat separations results for with **DS**.

DISCUSSION

Dynamic table-position-specific shimming is able to correct the static off-resonance ΔB_0 optimally along the full extent of the body in CMT MRI. Our current implementation was limited to demonstrating CMT dynamic shimming in 5 slices by high computation times required for the image reconstructions, fat/water separation and shim calculations (Total **NS** scan- **DS** scan time was ~13 minutes with computations performed on a 8Gb RAM, 1.66 GHz processor laptop). With higher computing power, future implementations should resolve this limitation.

REFERENCE 1. Brennan DD et al, AJR, 185, 418 (2005) 2. Berglund, J et al, MRM 63, 1659 (2010) 3. Bömert et al. JMIR 28, 1 (2008) 4. Sengupta et al, ISMRM 2014, pp 4249. 5. Berglund, J et al, MRM 67, 1684 (2012) 6. Hernando D, et al, MRM 67 638 (2012) 7. Sengupta S, et al, MRI 29 483 (2011).

ACKNOWLEDGEMENTS: R21 DK096282 from NIDDK/NIH & UL1 TR000445 from NCATS/NIH